Kavaljit H. Chhabra,[1] Jessica M. Adams,[1,2] Brian Fagel,[1] Daniel D. Lam,[1] Nathan Qi,[3] Marcelo Rubinstein,[1,4] and Malcolm J. Low[1,3]

Hypothalamic POMC Deficiency Improves Glucose Tolerance Despite Insulin Resistance by Increasing Glycosuria

Diabetes 2016;65:660–672 | DOI: 10.2337/db15-0804

Hypothalamic proopiomelanocortin (POMC) is essential for the physiological regulation of energy balance; however, its role in glucose homeostasis remains less clear. We show that hypothalamic arcuate nucleus (Arc)POMC-deficient mice, which develop severe obesity and insulin resistance, unexpectedly exhibit improved glucose tolerance and remain protected from hyperglycemia. To explain these paradoxical phenotypes, we hypothesized that an insulin-independent pathway is responsible for the enhanced glucose tolerance. Indeed, the mutant mice demonstrated increased glucose effectiveness and exaggerated glycosuria relative to wild-type littermate controls at comparable blood glucose concentrations. Central administration of the melanocortin receptor agonist melanotan II in mutant mice reversed alterations in glucose tolerance and glycosuria, whereas, conversely, administration of the antagonist Agouti-related peptide (Agrp) to wild-type mice enhanced glucose tolerance. The glycosuria of ArcPOMC-deficient mice was due to decreased levels of renal GLUT 2 (rGLUT2) but not sodium–glucose cotransporter 2 and was associated with reduced renal catecholamine content. Epinephrine treatment abolished the genotype differences in glucose tolerance and rGLUT2 levels, suggesting that reduced renal sympathetic nervous system (SNS) activity is the underlying mechanism for the observed glycosuria and improved glucose tolerance in ArcPOMC-deficient mice. Therefore, the ArcPOMC-SNS-rGLUT2 axis is potentially an insulin-independent therapeutic target to control diabetes.

Hypothalamic neurons integrate signals from metabolites such as pyruvate (1), as well as from hormones such as insulin (2,3), leptin (4), and GLP-1 (5) in the central nervous system control of glucose homeostasis. Disruption of hypothalamic leptin and insulin signaling leads to insulin resistance (6), indicating a physiological role of the hypothalamus in blood glucose regulation. Moreover, leptin receptors in hypothalamic proopiomelanocortin (POMC) neurons regulate glycemia independently of changes in food intake (7). Of note, POMC neurons directly sense glucose, and this property is impaired in obesity (8,9). Recently, Williams et al. (10) and Smith et al. (11) identified the contribution of X-box binding protein 1 and S6K1, respectively, in POMC neurons in the regulation of insulin sensitivity and hepatic glucose production. Overall, these studies and others validate POMC neurons as a potential therapeutic target to control hyperglycemia.

The melanocortin (MC) system, which originates in the POMC neurons, regulates energy balance through the MC3 receptor (MC3R) and MC4 receptor (MC4R). MC4R mutations cause hyperphagia, increased body weight, and insulin resistance in mice and humans (12–14). In contrast, MC3R-deficient mice exhibit a mild obesity syndrome associated with defects in nutrient partitioning despite normal food intake and energy expenditure (15,16). Mice lacking both MC4R and MC3R are significantly heavier than MC4R knockout mice, suggesting that these receptors play nonredundant roles in the regulation of energy balance (15). MC4R-deficient mice do not exhibit

[1]Department of Molecular and Integrative Physiology, University of Michigan Medical School, Ann Arbor, MI
[2]Neuroscience Graduate Program, University of Michigan, Ann Arbor, MI
[3]Department of Internal Medicine, Division of Metabolism, Endocrinology and Diabetes, University of Michigan Medical School, Ann Arbor, MI
[4]Instituto de Investigaciones en Ingeniería Genética y Biología Molecular, Consejo Nacional de Investigaciones Científicas y Técnicas, and Facultad de Ciencias Exactas y Naturales, Universidad de Buenos Aires, Buenos Aires, Argentina
Corresponding author: Malcolm J. Low, mjlow@umich.edu.

Received 11 June 2015 and accepted 7 October 2015.
This article contains Supplementary Data online at http://diabetes.diabetesjournals.org/lookup/suppl/doi:10.2337/db15-0804/-/DC1.

© 2016 by the American Diabetes Association. Readers may use this article as long as the work is properly cited, the use is educational and not for profit, and the work is not altered.

See accompanying article, p. 548.

fasting hyperglycemia or impaired glucose tolerance—the hallmark symptoms of diabetes—despite insulin resistance and obesity (12,13). Clinical data (14) also support this observation, suggesting that an insulin-independent pathway could be responsible for maintaining normoglycemia in subjects lacking MC signaling.

The POMC polypeptide is synthesized mainly in the pituitary gland and the hypothalamic arcuate nucleus (Arc). POMC negatively regulates energy homeostasis (17–19), and consequently, ArcPOMC deficiency causes obesity due to hyperphagia and decreased energy expenditure (19). Although the physiological significance of central POMC in body weight (19) and blood pressure (20) regulation is well established, its role in maintaining glucose homeostasis is less defined. Central *Pomc* expression is secondarily reduced in leptin-deficient obese *ob/ob* and leptin receptor–deficient diabetic *db/db* mice (21), suggesting the involvement of POMC in leptin-associated obesity and diabetes. Restoration of *Pomc* expression in *ob/ob* (22) and obese *Pomc* knockout mice (19) has been demonstrated to improve glucose tolerance and/or fasting glycemia; however, these studies did not take into account the secondary effects of obesity because the experiments were carried out in mice that were obese and/or concurrently hyperglycemic. Moreover, an abnormal counterregulatory response to hypoglycemia has been reported in global POMC-null mice (23), which lack peripheral as well as central MC signaling, but the specific function of hypothalamic POMC in glucose homeostasis remains to be established. In this study, we used ArcPOMC-deficient mice (19) generated by our laboratory to further determine the function of hypothalamic POMC in the regulation of glycemia. We measured glucose and insulin tolerance in groups of mutant mice that were either obese or weight matched to wild-type controls by food restriction to exclude secondary effects of obesity.

RESEARCH DESIGN AND METHODS

Study Approval

All procedures were approved by the University Committee on the Use and Care of Animals at the University of Michigan and followed the Public Health Service guidelines for the humane care and use of experimental animals.

Animal Care

Mice were housed in ventilated cages under a controlled temperature (~23°C) and photoperiod (12-h light/dark cycle, lights on from 6:00 A.M. to 6:00 P.M.) and fed tap water and laboratory chow (5L0D; LabDiet) containing 28.5 kcal% protein, 13.5 kcal% fat, and 58.0 kcal% carbohydrate either available ad libitum or restricted according to the approved experimental protocol. Weight-matched ArcPOMC-deficient mice were fed 75–80% of the daily total food consumed by wild-type littermates starting immediately after weaning to prevent development of obesity. Wild-type and mutant mice were housed individually for experiments involving weight matching.

Generation and Breeding of Mice

ArcPOMC-deficient mice were generated and bred as described previously (24). These mice have an identical phenotype to those described by Bumaschny et al. (19) because of the transcriptional blocking effects of a neoR cassette inserted in the neural enhancer region of the *Pomc* gene. However, they also have deletions of both nPE1 and nPE2, as shown in Supplementary Fig. 3 of the previous report (24). These mice have no detectable *Pomc* expression in the Arc but intact expression in the nucleus tractus solitarius and the pituitary gland. The mutant strain was backcrossed for at least five generations onto the C57BL/6J genetic background, and these incipient congenic mice were used throughout the study but are not included in the results presented in Fig. 2. Those experiments used mutant and wild-type littermates derived from the founding chimera after at least five generations of backcrossing to the 129S6/SvEvTac genetic background.

Oral Glucose and Intraperitoneal Insulin Tolerance Tests

Mice were fasted on separate occasions for 6 h (8:00 A.M.–2:00 P.M.) before being subjected to oral glucose tolerance and insulin tolerance tests. For oral glucose tolerance tests (OGTTs), glucose (fixed dose of 60 mg per mouse [G5767; Sigma]) was delivered into the stomach by an 18-gauge gavage needle (FNS-18-2; Kent Scientific Corporation), and blood was sampled at 0, 15, 30, 60, and 120 min for glucose measurements by an AlphaTRAK 2 glucometer. A fixed dose of glucose was given rather than a dose adjusted by body weight to eliminate the confounding effects of obesity. This method is recommended and has been validated for evaluating glucose tolerance in mice (25,26). Moreover, glucose tolerance in humans is assessed based on a fixed dose (75 g) of glucose administration. For experiments involving epinephrine (Fig. 7D), the OGTT was carried out 60 min after epinephrine 0.3 mg/kg lean mass i.p. or saline injection.

For insulin tolerance tests (ITTs), insulin 0.5 units/kg lean mass i.p. (Humulin R; Lilly) was administered and blood sampled at 0, 15, 30, 60, and 120 min for glucose measurements as described for OGTT. The total area under the curve (AUC) was calculated using the trapezoidal rule.

Frequently Sampled Intravenous Glucose Tolerance Test

A frequently sampled intravenous glucose tolerance test (FSIVGTT) (27) was performed in 6-h–fasted ArcPOMC-deficient mice or wild-type littermate controls 4 or 5 days after carotid arterial and jugular venous catheterization. The catheterizations were performed as described previously (28). Blood sampling was performed through the arterial catheter in unrestrained, conscious animals. A baseline fasted blood sample was obtained followed immediately by the intravenous administration of a fixed dose of 60 mg glucose per mouse over a period

of 20 s at t = 0 min. Blood was then sampled for measurement of glucose and insulin at t = 1, 2, 4, 7, 10, 15, 20, 30, and 60 min. The acute insulin response to hyperglycemia was based on the AUC of insulin levels between 0 and 10 min. The data were analyzed by the minimal model method to calculate glucose effectiveness as described previously (27,29) using MLAB software (Civilized Software Inc.).

Urine Glucose Levels

Urine glucose levels were measured by spot urine test (Bayer Diastix, 2803) during OGTTs at the various time points indicated in the Supplementary Data. For 24-h urine collections, mice were housed individually in metabolic cages (Tecniplast) and acclimatized to the cages for 1 week before undergoing experiments. Urine was collected for 24 h before and after OGTT, and the glucose concentration was quantified with an ADVIA 1800 Chemistry System (Siemens Healthcare, Tarrytown, NY) by a coupled enzymatic procedure with hexokinase and glucose-6-phosphate dehydrogenase.

Ten Percent Glucose Challenge Test

Mice were provided 10% glucose in drinking water for 24 h. Urine glucose concentration was quantified as just described.

Liver Glycogen Content and Pyruvate Tolerance Test

Hepatic glycogen levels were measured with a kit from Sigma (MAL016). For pyruvate tolerance tests (PTTs), sodium pyruvate (fixed dose of 60 mg per mouse [P5280; Sigma]) was injected intraperitoneally into mice after a 6-h fast, and blood glucose was measured at 0, 15, 30, 60, and 120 min postinjection.

Renal Epinephrine/Norepinephrine and Plasma Insulin Measurements

Mice were killed at 9:00 A.M., and the kidneys were collected under baseline (no treatment) conditions. Whole kidneys were homogenized in 0.01 N HCl, and the concentration of catecholamines was measured with ELISA as described by the manufacturer (BA E-5400; LDN). For plasma insulin measurements, mice were fasted for 6 h (8:00 A.M.–2:00 P.M.) before collecting blood from the tail vein with Fisherbrand Microhematocrit Capillary Tubes (22-362566). The blood was centrifuged at 4°C for 20 min at 2,000g, and the plasma was assayed with an Ultra Sensitive Mouse Insulin ELISA Kit (90080; Crystal Chem).

Intracerebroventricular Melanotan II and Agrp Treatments

Mice were anesthetized with 2–4% isoflurane. Twenty-six–gauge stainless steel guide cannulae cut 2.5 mm below the pedestal (Plastics One, Roanoke, VA) were implanted stereotaxically into the left lateral ventricle (anteroposterior −0.5 mm, mediolateral −1.0 mm, dorsoventral −2.0 mm relative to bregma), secured to the skull with screws (Small Parts) and dental cement, and occluded with stainless steel dummy obturators. Mice were then housed individually for 7–10 days for recovery. Melanotan II (MTII) 0.5 μg (M8693; Sigma) or Agrp 1 μg (003-57; Phoenix Pharmaceuticals, Inc.) were injected intracerebroventricularly three times daily in a volume of 5 μL over 5 min using a 33-gauge stainless steel injection cannula extending 0.5 mm below the guide cannula and connected to a 25-μL Hamilton syringe with polyethylene tubing. The last dose was administered 30 min before OGTT.

Western Blot

Mouse kidneys were harvested 60 min after oral glucose administration (fixed dose 60 mg) for the determination of differences in GLUT2 or sodium–glucose cotransporter (SGLT2) levels between genotypes. For experiments involving saline or epinephrine treatment, the kidneys were removed 60 min after the treatment and immediately frozen on dry ice. The renal cortical tissue was separated from the medullary portion with a razor blade under a dissecting microscope and suspended in 10 times volume ice-cold RIPA buffer (89900; Pierce) containing protease inhibitors (87786; Pierce). The tissue was minced with scissors and further homogenized with an Omni tissue homogenizer. The homogenate was centrifuged for 20 min at 12,000 rpm at 4°C in a microcentrifuge and the pellet discarded. The supernatant was analyzed for protein concentration by bicinchoninic acid assay (23227; Pierce, Thermo Scientific). The lysate containing 50 mg protein was mixed with an equal volume of Laemmli sample buffer (161-0737; Bio-Rad) before heating at 95°C for 10 min. SDS-PAGE was performed on TGX 4–20% gradient gels (456-1094; Bio-Rad) followed by a semidry transfer of the proteins onto polyvinylidene fluoride membranes (Millipore). The membranes were blocked in 5% nonfat dry milk solution in Tris-buffered saline with Tween 20 (TBST) for 1 h before incubating with primary antibodies overnight at 4°C. Rabbit polyclonal anti-GLUT2 serum (100-401-GN3 [Rockland Immunochemicals] or 07-1402 [Millipore]) and anti-GLUT2 affinity purified (600-401-GN3; Rockland Immunochemicals) and goat polyclonal anti-SGLT2 (sc-47402; Santa Cruz Biotechnology) antibodies were diluted 1:2,000 and 1:1,000, respectively, in TBST containing 5% powdered milk. After incubation, membranes were washed three times (15 min/wash) with TBST. After the washes, membranes were incubated with the secondary antibodies anti-rabbit (NA934; GE Healthcare) or anti-goat IgGs (sc-2768; Santa Cruz Biotechnology) coupled to horseradish peroxidase. Vinculin expression was evaluated on the same membranes to confirm equal sample loading using ab73412 antibody (Abcam). Luminescence was generated with the Amersham ECL Advance Western Blotting Detection Kit (GE Healthcare) and recorded on an imaging system. The correct band size (50 kDa) for GLUT2 was confirmed using a human embryonic kidney 293 cell lysate transfected with a GLUT2 expression vector (sc-120518; Santa Cruz Biotechnology) as

a positive control. We also confirmed the data with anti-GLUT2 serum provided by the laboratory of Bernard Thorens. GLUT2 antibodies used in this study identified nonspecific bands at 75 and 120 kDa in kidney samples.

Statistics

All data are presented as mean ± SEM and were analyzed by Student unpaired two-tailed or Welch *t* test or by two-way ANOVA followed by Bonferroni test when appropriate with GraphPad Prism 6 software. Some data, as identified in the figures, were log-transformed to convert them into a normal distribution. $P < 0.05$ was considered significant.

RESULTS

Obese and Weight-Matched ArcPOMC-Deficient Mice Exhibit Improved Glucose Tolerance Compared With Wild-Type Littermates

We measured fasting plasma insulin and determined whole-body insulin sensitivity in obese ArcPOMC-deficient mice (Fig. 1*A*). The ArcPOMC-deficient mice exhibited hyperinsulinemia and reduced insulin sensitivity compared with wild-type littermates (Fig. 1*B–D*). Additionally, the mutant mice had a higher HOMA insulin resistance (HOMA-IR) index (male 169.1 ± 35 vs. 9.0 ± 2 mmol/L · mU/L, female 165.3 ± 35 vs. 8.5 ± 2.3 mmol/L · mU/L, $P <$ 0.001), which is highly correlated with reduced insulin

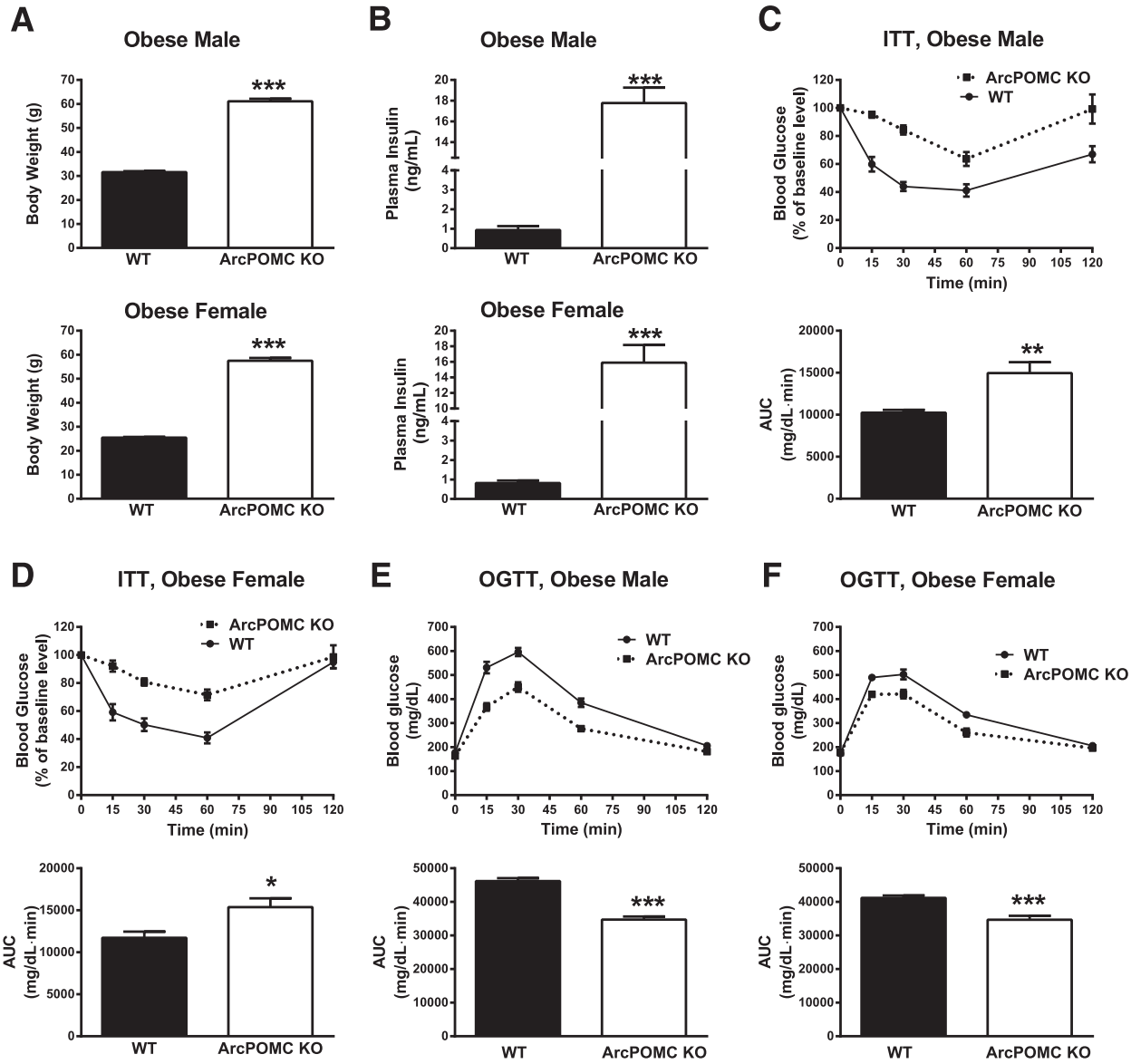

Figure 1— Improved glucose tolerance despite insulin resistance in C57BL/6J background 24-week-old obese ArcPOMC-deficient mice. *A*: Body weight. *B*: Fasting plasma insulin levels. *C* and *D*: ITT. *E* and *F*: OGTT. Bar graphs in *C*, *D*, *E*, and *F* represent the corresponding AUCs. Two-tailed Student *t* test was used for comparisons. *$P < 0.05$, **$P < 0.01$, ***$P < 0.001$ ($n = 6$). Error bars are mean ± SEM. KO, knockout; WT, wild type.

sensitivity (25), than the control group. These results are consistent with previous reports that suggested a role for central MCs in the regulation of insulin action (12–14). Next, we performed OGTTs, the most reliable method to assess glucose tolerance in mice (25). Paradoxically, we observed improved rather than impaired glucose tolerance in obese ArcPOMC-deficient mice (Fig. 1*E* and *F*), despite their insulin resistance. Furthermore, 52-week-old ArcPOMC-deficient mice did not exhibit fasting hyperglycemia or impaired glucose tolerance (data not shown) despite obesity, hyperphagia, and insulin resistance. The phenotype of improved glucose tolerance in the presence of reduced insulin sensitivity was also confirmed in obese 129S6 background ArcPOMC-deficient mice (Fig. 2).

To eliminate confounding or secondary effects of obesity that might have affected insulin and glucose metabolism in ArcPOMC-deficient mice, we determined insulin sensitivity and performed OGTTs with ArcPOMC-deficient mice weight-matched to wild-type littermates by calorie restriction (Fig. 3*A*). Fasting plasma insulin was significantly higher and insulin sensitivity lower in weight-matched ArcPOMC-deficient mice (Fig. 3*B–D*) than in wild-type littermates. Moreover, consistent with the obese ArcPOMC-deficient mice, the weight-matched mutant mice also had a higher HOMA-IR index than the control groups (male 13.4 ± 1.8 vs. 7.3 ± 1.7 mmol/L · mU/L, female 12.0 ± 1.2 vs. 6.2 ± 1.1 mmol/L · mU/L, $P < 0.05$). These data suggest that insulin resistance in ArcPOMC-deficient

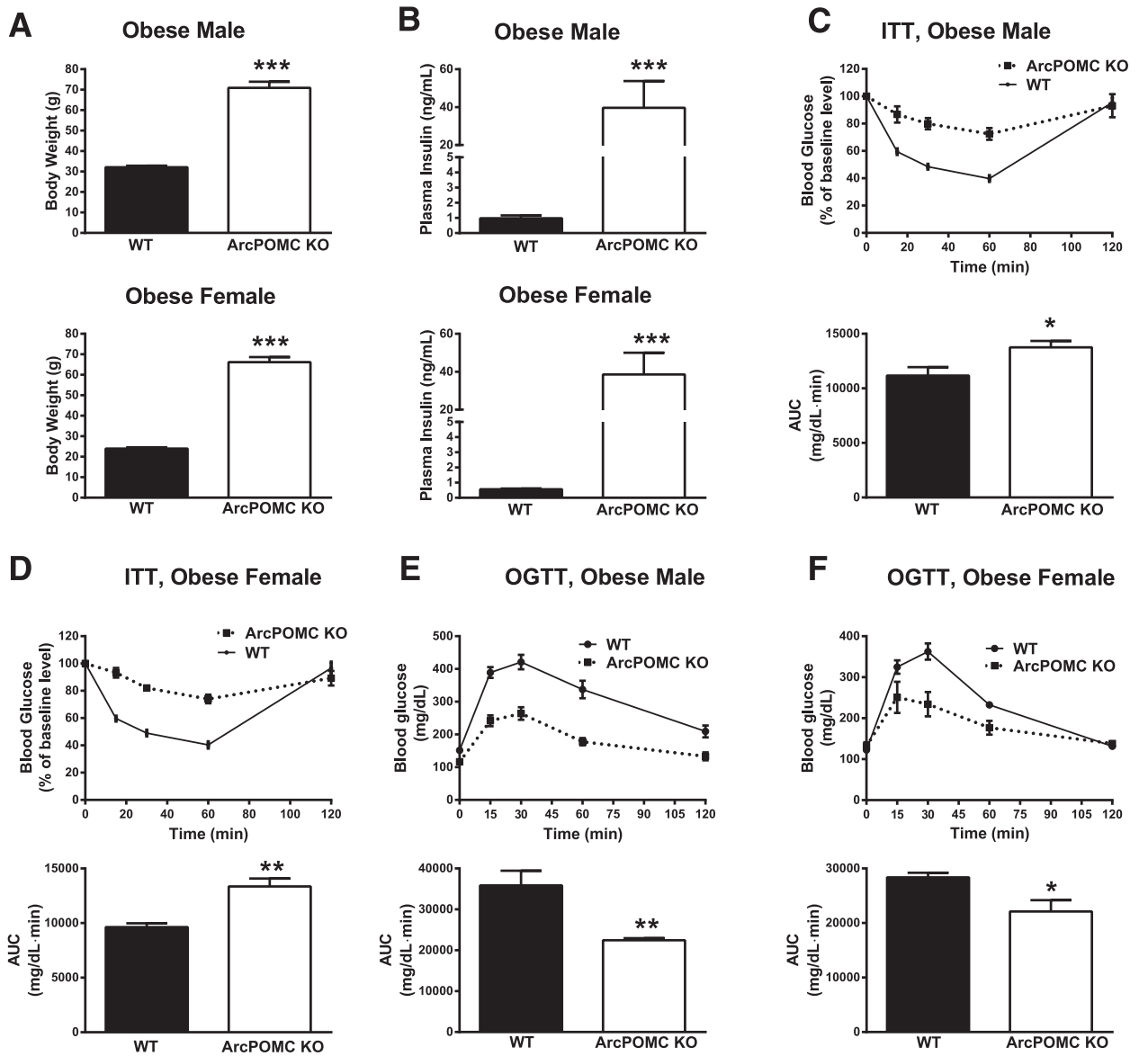

Figure 2—Evaluation of glucose homeostasis in 129S6/SvEvTac-background 24-week-old obese ArcPOMC-deficient mice. *A*: Body weight. *B*: Fasting plasma insulin levels. *C* and *D*: ITT. *E* and *F*: OGTT. Bar graphs in *C*, *D*, *E*, and *F* represent the corresponding AUCs. Two-tailed Student *t* test was used for comparisons. **P* < 0.05, ***P* < 0.01, ****P* < 0.001 (*n* = 6). Error bars are mean ± SEM. KO, knockout; WT, wild type.

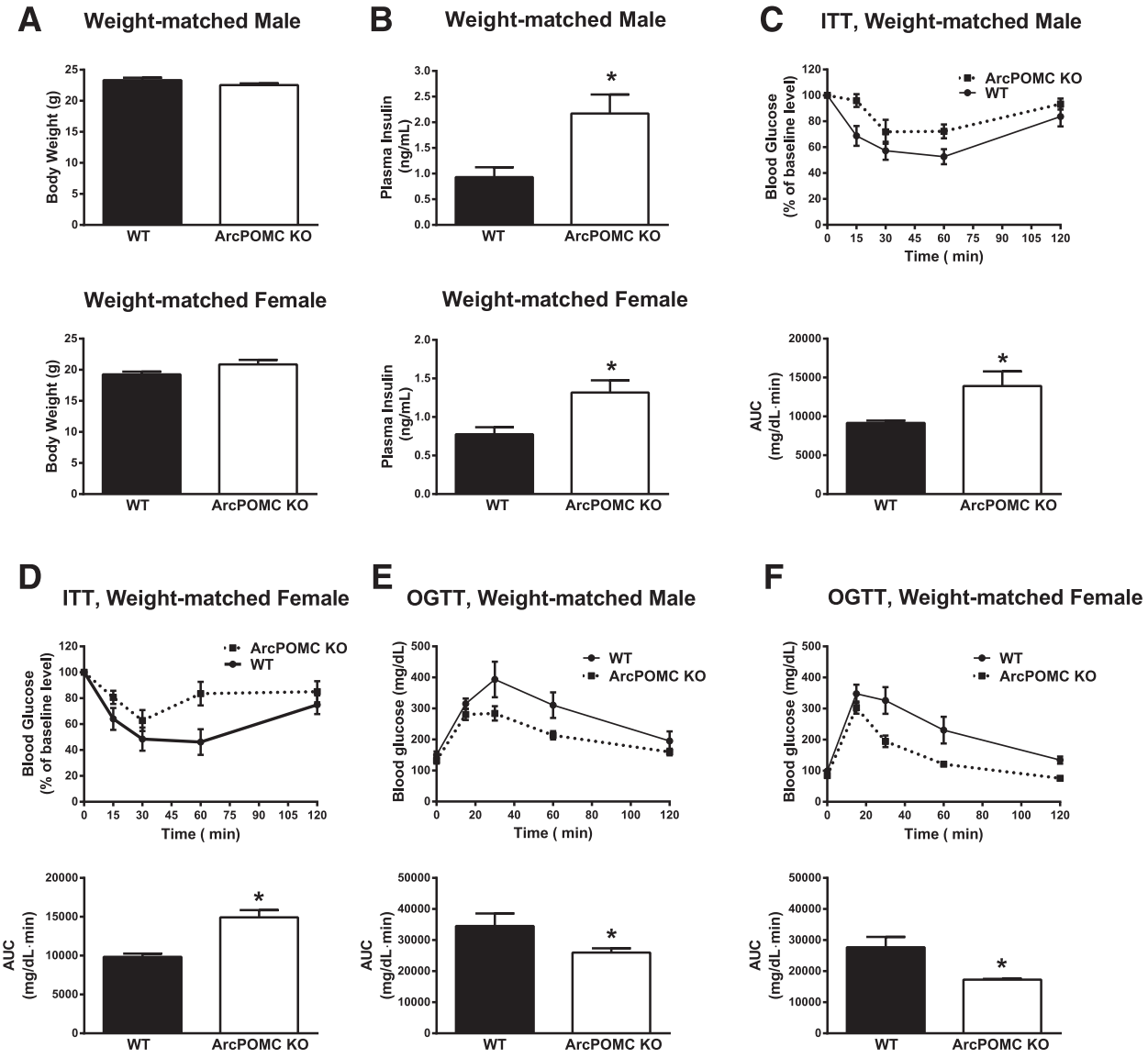

Figure 3—Improved glucose tolerance in the presence of insulin resistance in 12-week-old weight-matched ArcPOMC-deficient mice. *A*: Body weight. *B*: Fasting plasma insulin levels. *C* and *D*: ITT in weight-matched ArcPOMC-deficient mice. *E* and *F*: OGTT in weight-matched ArcPOMC-deficient mice. Bar graphs in *C*, *D*, *E*, and *F* represent the corresponding AUCs. Two-tailed Student *t* test was used for comparisons. $^*P < 0.05$ ($n = 6$). Error bars are mean ± SEM. KO, knockout; WT, wild type.

mice occurs independently of total body weight and is a direct outcome of ArcPOMC deficiency, similar to what has been observed in MC4R knockout mice that exhibit reduced insulin sensitivity even before the onset of obesity or hyperphagia (13). Despite their insulin resistance, the weight-matched ArcPOMC-deficient mice also showed improved glucose tolerance (Fig. 3*E* and *F*), indicating that the paradoxical phenotype is independent of changes in body weight and is a direct consequence of ArcPOMC deficiency. Moreover, 24-week-old weight-matched ArcPOMC-deficient mice exhibited improved glucose tolerance (data not shown), suggesting that the phenotype was independent of changes in age. However, weight-matched ArcPOMC-deficient mice have a mild persistent elevation in percentage of body fat composition measured by nuclear magnetic resonance (data not shown).

We performed an FSIVGTT (27,30) to determine whether the observed improvement of glucose tolerance in ArcPOMC-deficient mice depended on the route of administration. FSIVGTT data also revealed an improvement in glucose tolerance (Fig. 4*A* and *B*) in ad libitum–fed ArcPOMC-deficient mice (8 weeks old, 28 ± 0.6 g body weight) compared with the wild-type control group (8 weeks old, 22 ± 0.3 g body weight). The initial peak insulin concentration after glucose challenge was threefold higher than the baseline in wild-type mice; however, in mutant mice, the peak was only 1.3-fold higher than their already-elevated fasting insulin levels (Fig. 4*C*).

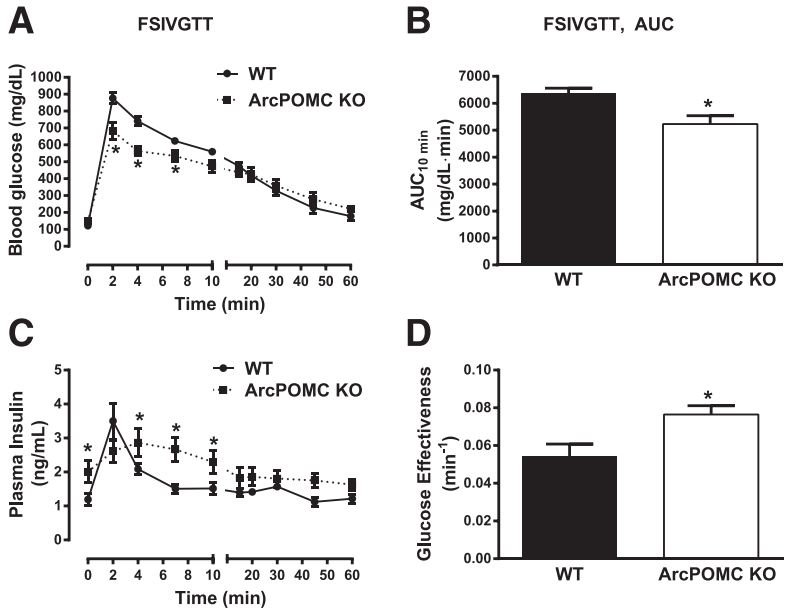

Figure 4—Improved glucose tolerance assessed by FSIVGTT in ArcPOMC-deficient mice. *A* and *B*: Blood glucose and corresponding AUCs of 0–10-min data points in 8-week-old ArcPOMC-deficient mice during FSIVGTT. *C* and *D*: Plasma insulin levels and glucose effectiveness in 8-week-old mice during FSIVGTT. Two-tailed Student *t* test was used for comparisons. **P* < 0.05 (*n* = 6 or 7). Error bars are mean ± SEM. KO, knockout; WT, wild type.

Consistent with results of FSIVGTT in *ob/ob* mice (27,30), ArcPOMC-deficient mice exhibited hyperinsulinemia (Fig. 4*C*) throughout the test, except for the initial peak, and hence, an elevated acute insulin response to glucose integrated over the first 10 min (674.3 ± 69 vs. 469.3 ± 52 μU/mL · min, $P < 0.05$), supporting the HOMA-IR data and confirming insulin resistance in the mutant mice as aforementioned. Of note, glucose effectiveness, defined as insulin-independent glucose disposal (30), was increased in the ArcPOMC-deficient mice (Fig. 4*D*) compared with wild-type littermates, suggesting that an insulin-independent mechanism mediates the improvement in glucose tolerance. These data confirm that the ArcPOMC-deficient mice exhibit improved glucose tolerance despite insulin resistance.

ArcPOMC-Deficient Mice Show Elevated Glycosuria but Normal Hepatic Glycogen Levels and Gluconeogenesis

To explain the paradox of improved glucose tolerance in the presence of insulin resistance, we hypothesized that ArcPOMC-deficient mice would exhibit exaggerated glycosuria—an insulin-independent mechanism of glucose disposal that is currently used as a therapy to control diabetes (31)—compared with wild-type littermates. To test this hypothesis, we analyzed urine glucose levels under various glucose-challenged conditions. Weight-matched ArcPOMC-deficient mice showed elevated glycosuria at all time points during OGTT compared with wild-type mice (Supplementary Table 1), even though their corresponding-blood glucose levels were lower than in wild-type mice (Fig. 3*E* and *F*). Moreover, urine from the mutant mice collected over 24 h in metabolic cages after OGTT showed a higher glucose concentration than that of the control group (Fig. 5*A*). To further confirm the reduced threshold for renal glucose reabsorption in the mutant mice, we provided 10% glucose in drinking water for 24 h and collected urine in metabolic cages. We found a profound increase in urinary glucose excretion by the mutant compared with the wild-type mice (Fig. 5*B*), further validating our hypothesis of suppressed renal glucose reabsorption in ArcPOMC-deficient mice. Obese ad libitum–fed ArcPOMC-deficient mice showed elevated glycosuria (93.5 ± 14 vs. 48 ± 5 mg/dL, $P < 0.05$) even without glucose challenge, unlike the calorie-restricted and weight-matched mice. Additionally, the obese mice but not the calorie-restricted mice exhibited albuminuria (10.4 ± 2.6 vs. 1.1 ± 0.5 μg/day, $P < 0.0001$) compared with the wild-type group, suggesting secondary effects of obesity on kidney pathology. Of note, both obese and weight-matched mutant mice had elevated natriuresis (0.5 ± 0.02 and 0.4 ± 0.03 mmol/day, respectively, vs. 0.3 ± 0.01 mmol/day; $P < 0.05$). Decreased renal sympathetic nervous system (SNS) activity in the mutant mice can possibly explain the observed natriuresis.

In addition to glycosuria, hepatic glycogen turnover and gluconeogenesis contribute to glucose homeostasis. Moreover, hypothalamic α-melanocyte-stimulating hormone regulates hepatic gluconeogenesis (32). Hence, we measured liver glycogen levels and evaluated gluconeogenesis by a PTT to determine whether changes in these parameters are responsible for protecting ArcPOMC-deficient mice against hyperglycemia in the presence

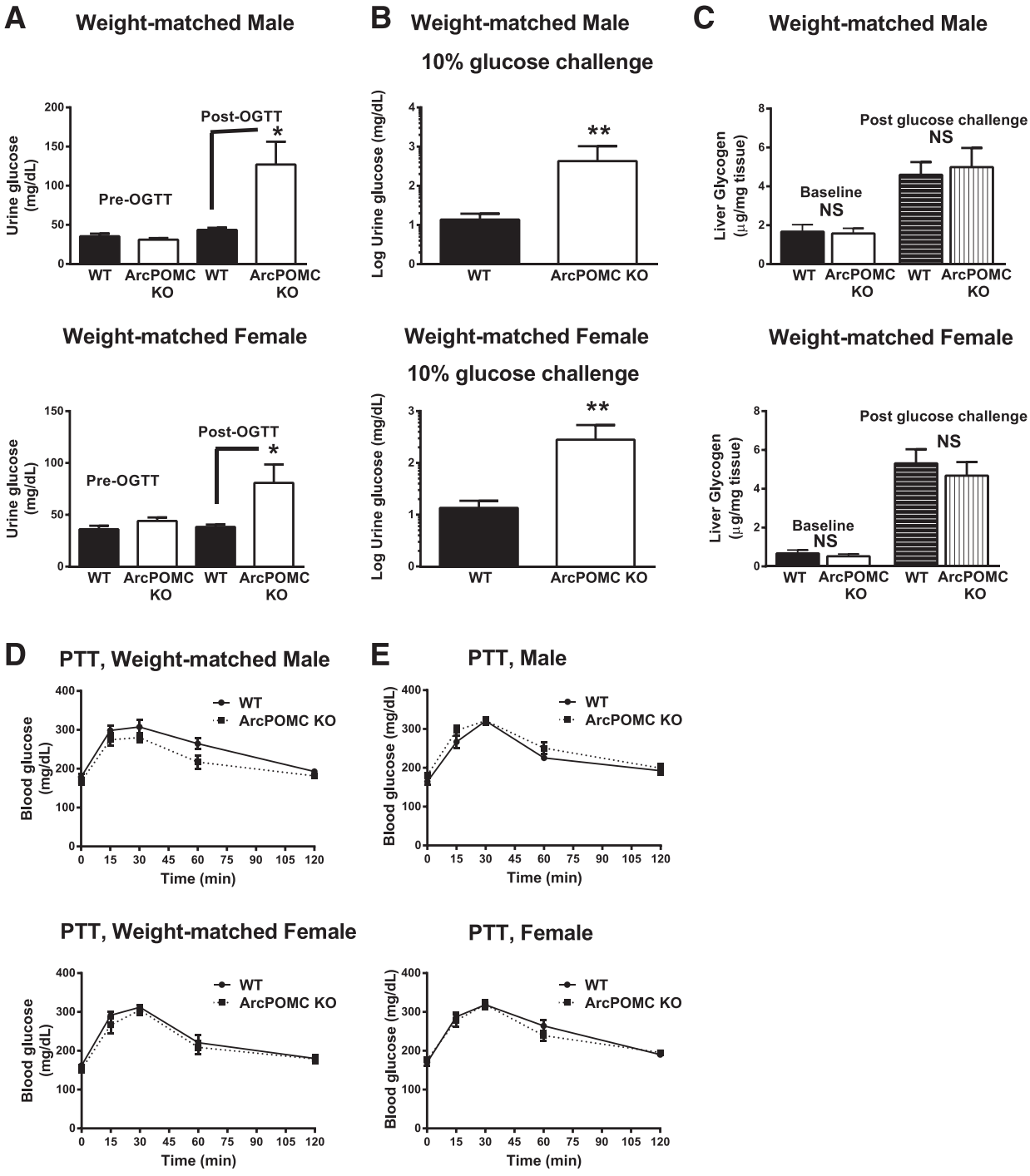

Figure 5—Elevated glycosuria, normal liver glycogen levels, and normal gluconeogenesis in weight-matched or obese ArcPOMC-deficient mice. *A*: Twenty-four-hour urine glucose concentration in weight-matched 12-week-old mice before and after OGTT. *B*: Twenty-four-hour urine glucose concentration in weight-matched 12-week-old mice that were challenged with 10% glucose provided in their drinking water. *C*: Fasting hepatic glycogen levels at baseline and after glucose challenge in weight-matched 8-week-old mice ($n = 6$). *D*: PTT in 8-week-old weight-matched mice ($n = 6$). *E*: PTT in 16-week-old obese mutant mice ($n = 6$). Two-tailed Student *t* test was used for comparisons. $^*P < 0.05$, $^{**}P < 0.01$ ($n = 6$ or 7). Error bars are mean ± SEM. KO, knockout; NS, not significant at $P > 0.05$; WT, wild type.

of insulin resistance. We found no differences in either hepatic glycogen levels (baseline and after glucose challenge) (Fig. 5*C*) or gluconeogenesis (PTT) (Fig. 5*D* and *E*) between ArcPOMC-deficient mice and wild-type littermates. Therefore, a reduced threshold for glucose reabsorption appears to be the major mechanism responsible for the enhanced glucose tolerance phenotype in ArcPOMC-deficient mice.

Pharmacological Experiments With MTII or Agrp Support Results From the ArcPOMC-Deficient Genetic Mouse Model

We treated ArcPOMC-deficient mice with MTII 0.5 μg/5 μL PBS i.c.v. t.i.d., a nonselective MC receptor agonist, to validate whether the phenotype of improved glucose tolerance and glycosuria is attributable to decreased MC signaling in POMC-deficient mice. MTII treatment reversed the phenotype and resulted in normal, rather than enhanced, glucose tolerance (Fig. 6*A*) concomitantly with the absence of exaggerated glycosuria (Supplementary Table 2) compared with the same set of mice after saline injections. Consistent with our previous study (33), MTII decreased food intake and body weight dramatically in the mutant mice (Fig. 6*B* and *C*). A wild-type group treated with MTII was not included in the study because our main goal was to ascertain whether MTII can reverse the phenotype of ArcPOMC-deficient mice.

To pharmacologically simulate the reduced central MC signaling of ArcPOMC-deficient mice, we treated wild-type mice with Agrp 1 μg/5 μL PBS i.c.v. t.i.d., an MC3/4R antagonist. Consistent with the results from the mutant mice, Agrp-treated wild-type mice had improved glucose tolerance (Fig. 6*A*) and elevated glycosuria (Supplementary Table 2) at 15- and 60-min intervals during OGTT relative to the same set of mice after saline administration. However, unlike the mutant mice, glycosuria was absent at the 120-min time point during OGTTs in Agrp-treated wild-type mice. As expected, Agrp increased body weight and food intake in wild-type mice (Fig. 6*B* and *C*).

ArcPOMC-Deficient Mice Have Reduced Renal GLUT2 but Not SGLT2 Levels

To determine the molecular mechanisms underlying exaggerated glycosuria in ArcPOMC-deficient mice, we evaluated the expression of the major renal (r) proximal tubule glucose transporters GLUT2 and SGLT2 60 min after oral glucose administration (fixed dose 60 mg per mouse). We observed a significant decrease in rGLUT2 but not rSGLT2 protein levels (Fig. 7*A* and *B*) in the mutant mice, suggesting that suppression of rGLUT2 mediates glycosuria in ArcPOMC-deficient mice.

Epinephrine Abolishes the Genotype Differences Between Wild-Type and ArcPOMC-Deficient Mice

Because of the enriched sympathetic innervation of kidneys (34) and the demonstrated direct relationship between central POMC signaling and sympathetic outflow (35–37), we questioned whether reduced sympathetic tone contributes to the observed downregulation of rGLUT2 in ArcPOMC-deficient mice. We found that kidney norepinephrine and epinephrine levels were decreased by 50% in the mutant mice compared with the controls (Fig. 8*A*) consistent with a previous clinical report (38) that demonstrated reduced sympathetic outflow in patients with MC signaling deficiency. To confirm the role of the SNS in the regulation of renal glucose reabsorption, we treated both wild-type and ArcPOMC-deficient mice with epinephrine 0.3 mg/kg lean mass i.p. or saline and assessed rGLUT2 expression 60 min later. We found that epinephrine treatment increased rGLUT2 expression in the mutant and wild-type mice (Fig. 8*B* and *C*).

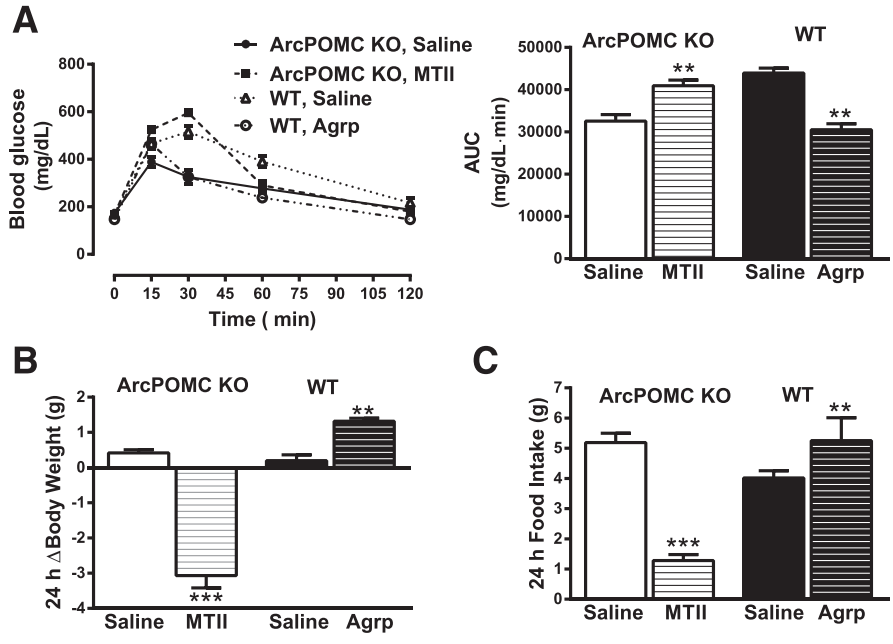

Figure 6—MTII and Agrp treatment in female ArcPOMC-deficient and wild-type mice, respectively. *A*: OGTT in ArcPOMC-deficient and wild-type mice (bar graphs represent AUC). *B*: Twenty-four-hour body weight change after MTII or Agrp treatment. *C*: Twenty-four-hour food intake. Two-tailed Student paired *t* test was used for comparisons. $^{**}P < 0.01$, $^{***}P < 0.001$ ($n = 6$). Error bars are mean ± SEM. KO, knockout; WT, wild type.

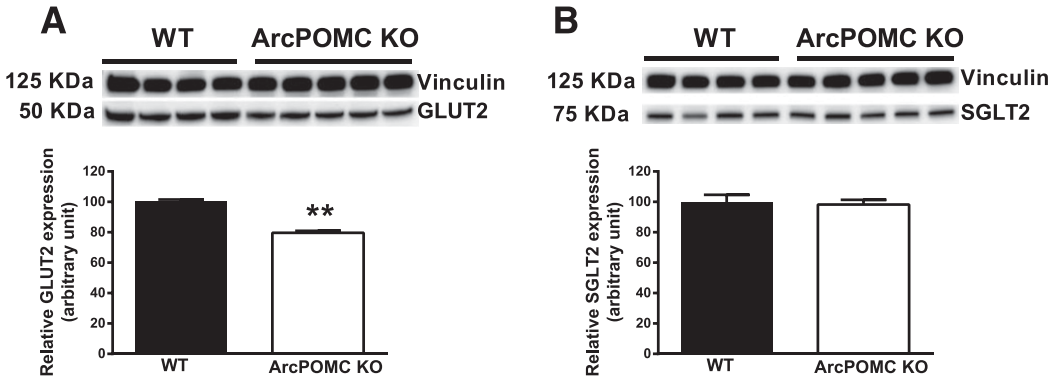

Figure 7—Reduced rGLUT2 but not rSGLT2 levels in ArcPOMC-deficient mice. *A* and *B*: Representative Western blot images of renal cortical GLUT2 and SGLT2, respectively (n = 8 per group for bar graphs that represent relative expression). Two-tailed Student t test was used for comparisons. $^{**}P < 0.01$. Error bars are mean ± SEM. KO, knockout; WT, wild type.

Epinephrine treatment also abolished the differences in glucose tolerance (Fig. 8*D*) between ArcPOMC-deficient and wild-type mice. Moreover, after epinephrine treatment, none of the mutant mice showed glycosuria at 60 and 120 min during OGTT (Supplementary Table 1), supporting our hypothesis that mutant mice show elevated glycosuria because of low sympathetic tone. These data corroborate a previous report (39) that suggested a role of the SNS in regulating renal glucose reabsorption and rGLUT2 in rats.

DISCUSSION

In this study, we examined the role of hypothalamic POMC in the regulation of glucose homeostasis. Given the influence of genetics on energy homeostasis in mice (40), we assessed the phenotype of ArcPOMC-deficient mice on both C57BL/6 and 129S6 genetic backgrounds. We were surprised to find an improvement in glucose tolerance in ArcPOMC-deficient mice on both backgrounds. Moreover, the mutant mice had normal fasting glycemia despite obesity and insulin resistance. These data are consistent with previous observations that MC4R-deficient humans and mice exhibit normoglycemia despite obesity (12–14). The current data also suggest that hypothalamic POMC regulates plasma insulin levels and insulin sensitivity independently of changes in body weight, thereby supporting the observation by Fan et al. (13) that central MCs directly control serum insulin levels. Moreover, the findings that central MC signaling regulates hepatic and muscle insulin sensitivity (41,42) might explain the exacerbated insulin resistance in the ArcPOMC-deficient mice.

The FSIVGTT data showed an increase in glucose effectiveness (insulin-independent glucose disposal) in ArcPOMC-deficient mice, which supports a study by Morton et al. (30) demonstrating a role of the brain in enhancing glucose tolerance independently of insulin action. Elevated glycosuria might explain the increased insulin-independent glucose disposal in ArcPOMC-deficient mice. Indeed, an increase in glycosuria in the mutant mice relative to wild-type littermates was observed. Elevated glycosuria in the absence of hyperglycemia in ArcPOMC-deficient mice suggests that hypothalamic POMC regulates the renal glucose threshold. The normal average renal glucose threshold for mice is 400 mg/dL (43); however, ArcPOMC-deficient mice exhibited elevated glycosuria (Supplementary Table 1) at average blood glucose levels of 230 and 180 mg/dL at 60 and 120 min, respectively, during OGTT (Fig. 3*E* and *F*). MTII treatment decreased glycosuria in the mutant mice, indicating a direct role of the central MC system in the regulation of glucose reabsorption. In contrast, Agrp increased glycosuria at 15 and 60 min but not at 120 min during OGTTs in wild-type mice. This discrepancy may be attributed to short-term Agrp treatment and/or a mechanism other than glycosuria, such as increased insulin sensitivity, that might be partly responsible for Agrp-mediated improvement in glucose tolerance.

We assessed rSGLT2 levels in ArcPOMC-deficient mice because glycosuria induced by pharmacological inhibition of rSGLT2 is a novel strategy to combat hyperglycemia in patients with diabetes (31), but the mutant mice surprisingly exhibited normal rSGLT2 levels. However, rGLUT2 was reduced in the mutant mice by 20%, indicating that GLUT2 deficiency mediates elevated glycosuria in ArcPOMC-deficient mice. Indeed, GLUT2 deficiency or gene mutations are linked to glycosuria in rodents (44) and humans even in the absence of hyperglycemia (45). We did not examine rSGLT2 or rGLUT2 intracellular trafficking in the mutant mice. It is possible that defective trafficking of the glucose transporters between cytoplasmic vesicles and the plasma membrane could be partly responsible for the elevated glycosuria in ArcPOMC-deficient mice. Future studies are needed to elucidate this possibility.

MTII and epinephrine abrogated the genotype differences in glucose tolerance and glycosuria, suggesting that suppressed SNS activity due to inadequate central MC

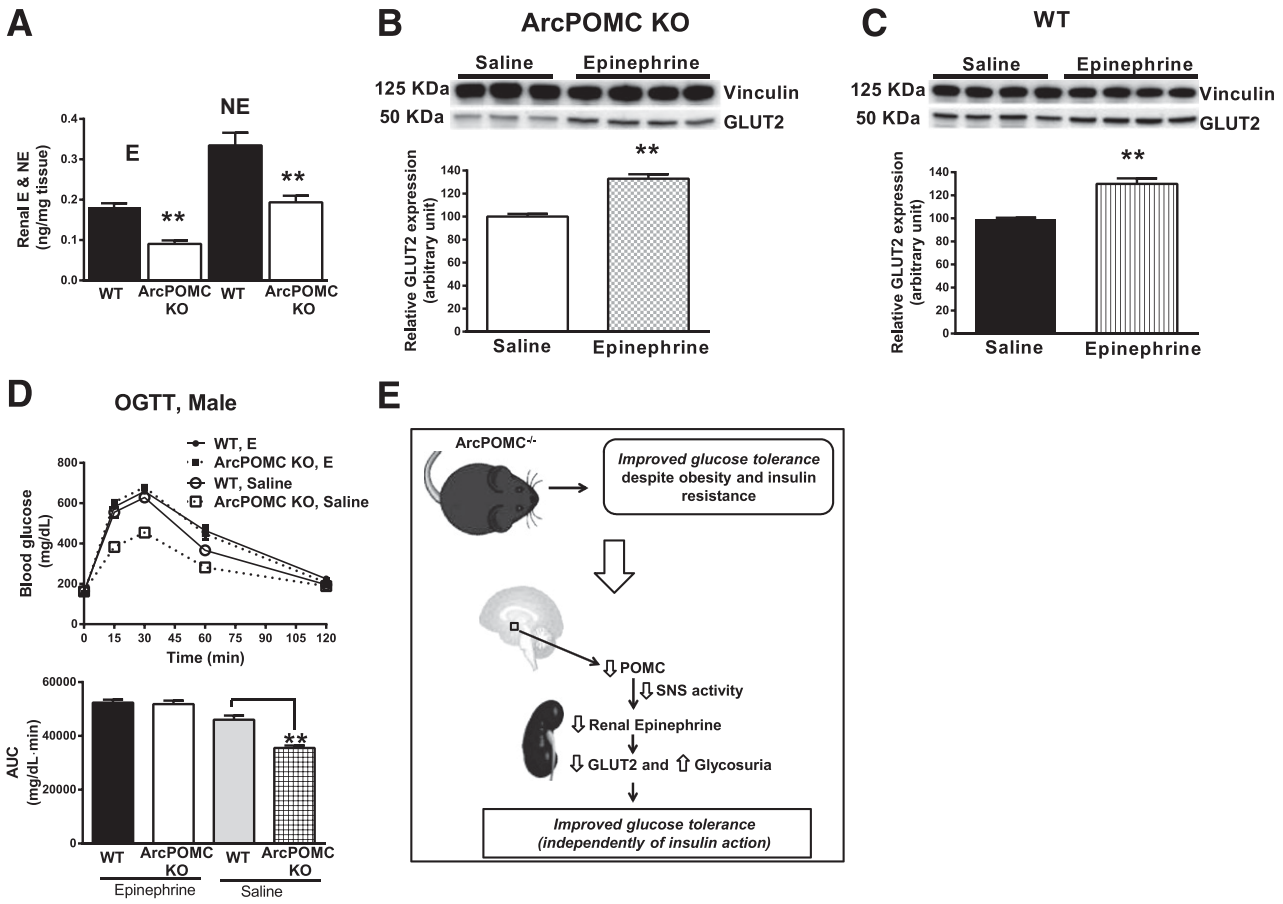

Figure 8—ArcPOMC regulates rGLUT2 through the SNS. *A*: Whole-kidney epinephrine and norepinephrine levels (n = 6). *B*: Renal cortical GLUT2 expression in the presence of epinephrine treatment in ArcPOMC-deficient mice. *C*: Renal cortical GLUT2 expression in the presence of epinephrine treatment in wild-type mice (n = 8 per group for bar graphs that represent relative expression). *D*: OGTT in epinephrine- or saline-treated mice (n = 6 per group) [genotype effect: $F(1,23) = 20.2$, $P = 0.0002$; treatment effect: $F(1,23) = 84.9$, $P < 0.0001$]. *E*: Proposed insulin-independent mechanism by which hypothalamic POMC deficiency improves glucose tolerance. Two-tailed Student t test or two-way ANOVA followed by Bonferroni multiple comparisons test were used for comparisons. $^{**}P < 0.01$. Error bars are mean ± SEM. E, epinephrine; KO, knockout; NE, norepinephrine; WT, wild type.

signaling is the underlying mechanism for elevated glycosuria in ArcPOMC-deficient mice. The finding that epinephrine controls rGLUT2 levels and thus renal glucose reabsorption might partly explain the reduced fasting glycemia and normal glucose tolerance in the presence of insulin resistance in epinephrine/norepinephrine knockout mice (46). Moreover, the observation that MC4R-deficient mice (13) and humans (14) exhibit normal blood glucose levels despite obesity and insulin resistance might be attributed to suppressed rGLUT2 expression because of decreased renal sympathetic tone (38,47). Greenfield et al. (38) demonstrated the presence of suppressed sympathetic activity and thus reduced blood pressure in obese MC4R-deficient subjects, thereby confirming the preclinical data reported in MC4R knockout mice (47). Hence, it is possible that epinephrine/norepinephrine- and MC4R-deficient mice, like ArcPOMC-deficient mice in the current study, exhibit exaggerated glycosuria because of suppressed rGLUT2 expression mediated by low sympathetic tone. Elevated glycosuria attributed to low sympathetic tone could also be one of the reasons why renal denervation improves glycemia in patients with hypertension (48).

In summary, we have identified a previously unrecognized hypothalamic-SNS-renal axis (Fig. 8*E*) that controls glucose homeostasis by regulating proximal tubular glucose reabsorption and that complements other recently reported brain-mediated insulin-independent mechanisms of glycemia regulation (30,49). The SNS-mediated increased glucose reabsorption may be of physiological relevance during fight-or-flight responses to prevent glucose (energy) loss in urine and would complement other sympathetic actions on glucose homeostasis, including inhibition of insulin secretion from β-cells and increased glucose production by the liver to meet increased metabolic demand under stress. This pathway (Fig. 8*E*) also predicts that renal-specific antagonism of GLUT2 is an alternative, or possibly synergistic therapeutic approach,

to SGLT2 antagonism for diabetes control even in the presence of insulin resistance and obesity.

Acknowledgments. The authors thank Lisa Harrison-Bernard (Louisiana State University Health Sciences Center, New Orleans, LA) and Frank Brosius (University of Michigan, Ann Arbor, MI) for expert advice; Karin Abarca Heidemann, Angela Gilmore, and their team at Rockland Immunochemicals Inc. (Pottstown, PA) for providing a new affinity-purified GLUT2 antibody that was developed with the support of a 2014 Joy Cappel Young Investigator Award to K.H.C.; Eva Yokosawa and Courtney Attard (Low Laboratory, University of Michigan) for mouse breeding and genotyping; Bernard Thorens and Salima Metref (Center for Integrative Genomics, University of Lausanne, Lausanne, Switzerland) for providing the GLUT2 antibody; Dalbir Kaur Chhabra (University of New Orleans, New Orleans, LA) for assistance with MLAB; Melanie Schmitt and Elizabeth Limback (University of Michigan) for help with FSIVGTTs; and members of the Low Laboratory (University of Michigan) for their valuable suggestions on this project.

Funding. This work was supported by National Institutes of Health (NIH) early stage neurosciences training grant T32-NS-076401 (to J.M.A.) and summer fellowship grant R25-DK-088752 (to B.F.), American Heart Association grants 11POST7430087 and 13POST16890000 (to D.D.L.), and NIH grants R01-DK-068400 (to M.R. and M.J.L.) and R01-DK-066604 (to M.J.L.). This work used core services provided by the University of Michigan Animal Phenotyping and Chemistry Cores supported by the Michigan Diabetes Research Center and the Michigan Nutrition and Obesity Research Center (NIH grants P30-DK-020572 and P30-DK-089503).

Duality of Interest. No potential conflicts of interest relevant to this article were reported.

Author Contributions. K.H.C. contributed to the study concept and design, performance of experiments, data analysis, and writing and editing of the manuscript. J.M.A., B.F., D.D.L., and N.Q. contributed to the performance of experiments and editing of the manuscript. M.R. contributed to the discussion and editing of the manuscript. M.J.L. contributed to the study concept and design, data analysis, and writing of the manuscript. M.J.L. is the guarantor of this work and, as such, had full access to all the data in the study and takes responsibility for the integrity of the data and the accuracy of the data analysis.

References

1. Lam TK, Gutierrez-Juarez R, Pocai A, Rossetti L. Regulation of blood glucose by hypothalamic pyruvate metabolism. Science 2005;309:943–947
2. Gelling RW, Morton GJ, Morrison CD, et al. Insulin action in the brain contributes to glucose lowering during insulin treatment of diabetes. Cell Metab 2006;3:67–73
3. Obici S, Zhang BB, Karkanias G, Rossetti L. Hypothalamic insulin signaling is required for inhibition of glucose production. Nat Med 2002;8:1376–1382
4. Coppari R, Ichinose M, Lee CE, et al. The hypothalamic arcuate nucleus: a key site for mediating leptin's effects on glucose homeostasis and locomotor activity. Cell Metab 2005;1:63–72
5. Knauf C, Cani PD, Perrin C, et al. Brain glucagon-like peptide-1 increases insulin secretion and muscle insulin resistance to favor hepatic glycogen storage. J Clin Invest 2005;115:3554–3563
6. Hill JW, Elias CF, Fukuda M, et al. Direct insulin and leptin action on pro-opiomelanocortin neurons is required for normal glucose homeostasis and fertility. Cell Metab 2010;11:286–297
7. Berglund ED, Vianna CR, Donato J Jr, et al. Direct leptin action on POMC neurons regulates glucose homeostasis and hepatic insulin sensitivity in mice. J Clin Invest 2012;122:1000–1009
8. Parton LE, Ye CP, Coppari R, et al. Glucose sensing by POMC neurons regulates glucose homeostasis and is impaired in obesity. Nature 2007;449:228–232
9. Ibrahim N, Bosch MA, Smart JL, et al. Hypothalamic proopiomelanocortin neurons are glucose responsive and express K(ATP) channels. Endocrinology 2003;144:1331–1340
10. Williams KW, Liu T, Kong X, et al. Xbp1s in Pomc neurons connects ER stress with energy balance and glucose homeostasis. Cell Metab 2014;20:471–482
11. Smith MA, Katsouri L, Irvine EE, et al. Ribosomal S6K1 in POMC and AgRP neurons regulates glucose homeostasis but not feeding behavior in mice. Cell Reports 2015;11:335–343
12. Huszar D, Lynch CA, Fairchild-Huntress V, et al. Targeted disruption of the melanocortin-4 receptor results in obesity in mice. Cell 1997;88:131–141
13. Fan W, Dinulescu DM, Butler AA, Zhou J, Marks DL, Cone RD. The central melanocortin system can directly regulate serum insulin levels. Endocrinology 2000;141:3072–3079
14. Farooqi IS, Yeo GSH, Keogh JM, et al. Dominant and recessive inheritance of morbid obesity associated with melanocortin 4 receptor deficiency. J Clin Invest 2000;106:271–279
15. Chen AS, Marsh DJ, Trumbauer ME, et al. Inactivation of the mouse melanocortin-3 receptor results in increased fat mass and reduced lean body mass. Nat Genet 2000;26:97–102
16. Renquist BJ, Murphy JG, Larson EA, et al. Melanocortin-3 receptor regulates the normal fasting response. Proc Natl Acad Sci U S A 2012;109:E1489–E1498
17. Krude H, Biebermann H, Luck W, Horn R, Brabant G, Grüters A. Severe early-onset obesity, adrenal insufficiency and red hair pigmentation caused by POMC mutations in humans. Nat Genet 1998;19:155–157
18. Yaswen L, Diehl N, Brennan MB, Hochgeschwender U. Obesity in the mouse model of pro-opiomelanocortin deficiency responds to peripheral melanocortin. Nat Med 1999;5:1066–1070
19. Bumaschny VF, Yamashita M, Casas-Cordero R, et al. Obesity-programmed mice are rescued by early genetic intervention. J Clin Invest 2012;122:4203–4212
20. Dunbar JC, Lu H. Proopiomelanocortin (POMC) products in the central regulation of sympathetic and cardiovascular dynamics: studies on melanocortin and opioid interactions. Peptides 2000;21:211–217
21. Mizuno TM, Kleopoulos SP, Bergen HT, Roberts JL, Priest CA, Mobbs CV. Hypothalamic pro-opiomelanocortin mRNA is reduced by fasting and [corrected] in *ob/ob* and *db/db* mice, but is stimulated by leptin. Diabetes 1998;47:294–297
22. Mizuno TM, Kelley KA, Pasinetti GM, Roberts JL, Mobbs CV. Transgenic neuronal expression of proopiomelanocortin attenuates hyperphagic response to fasting and reverses metabolic impairments in leptin-deficient obese mice. Diabetes 2003;52:2675–2683
23. Hochgeschwender U, Costa JL, Reed P, Bui S, Brennan MB. Altered glucose homeostasis in proopiomelanocortin-null mouse mutants lacking central and peripheral melanocortin. Endocrinology 2003;144:5194–5202
24. Lam DD, de Souza FS, Nasif S, et al. Partially redundant enhancers cooperatively maintain mammalian POMC expression above a critical functional threshold. PLoS Genet 2015;11:e1004935
25. Andrikopoulos S, Blair AR, Deluca N, Fam BC, Proietto J. Evaluating the glucose tolerance test in mice. Am J Physiol Endocrinol Metab 2008;295:E1323–E1332
26. Ayala JE, Samuel VT, Morton GJ, et al.; NIH Mouse Metabolic Phenotyping Center Consortium. Standard operating procedures for describing and performing metabolic tests of glucose homeostasis in mice. Dis Model Mech 2010;3:525–534
27. Alonso LC, Watanabe Y, Stefanovski D, et al. Simultaneous measurement of insulin sensitivity, insulin secretion, and the disposition index in conscious unhandled mice. Obesity (Silver Spring) 2012;20:1403–1412
28. Adams JM, Otero-Corchon V, Hammond GL, Veldhuis JD, Qi N, Low MJ. Somatostatin is essential for the sexual dimorphism of GH secretion, corticosteroid-binding globulin production, and corticosterone levels in mice. Endocrinology 2015;156:1052–1065
29. Boston RC, Stefanovski D, Moate PJ, Sumner AE, Watanabe RM, Bergman RN. MINMOD Millennium: a computer program to calculate glucose effectiveness and insulin sensitivity from the frequently sampled intravenous glucose tolerance test. Diabetes Technol Ther 2003;5:1003–1015

30. Morton GJ, Matsen ME, Bracy DP, et al. FGF19 action in the brain induces insulin-independent glucose lowering. J Clin Invest 2013;123:4799–4808
31. Komoroski B, Vachharajani N, Feng Y, Li L, Kornhauser D, Pfister M. Dapagliflozin, a novel, selective SGLT2 inhibitor, improved glycemic control over 2 weeks in patients with type 2 diabetes mellitus. Clin Pharmacol Ther 2009; 85:513–519
32. Schneeberger M, Gómez-Valadés AG, Altirriba J, et al. Reduced α-MSH underlies hypothalamic ER-stress-induced hepatic gluconeogenesis. Cell Reports 2015;12:361–370
33. Tolle V, Low MJ. In vivo evidence for inverse agonism of Agouti-related peptide in the central nervous system of proopiomelanocortin-deficient mice. Diabetes 2008;57:86–94
34. DiBona GF, Kopp UC. Neural control of renal function. Physiol Rev 1997;77: 75–197
35. Sohn J-W, Harris LE, Berglund ED, et al. Melanocortin 4 receptors reciprocally regulate sympathetic and parasympathetic preganglionic neurons. Cell 2013;152:612–619
36. Berglund ED, Liu T, Kong X, et al. Melanocortin 4 receptors in autonomic neurons regulate thermogenesis and glycemia. Nat Neurosci 2014;17:911–913
37. Humphreys MH. Cardiovascular and renal actions of melanocyte-stimulating hormone peptides. Curr Opin Nephrol Hypertens 2007;16:32–38
38. Greenfield JR, Miller JW, Keogh JM, et al. Modulation of blood pressure by central melanocortinergic pathways. N Engl J Med 2009;360:44–52
39. Schaan BD, Irigoyen MC, Lacchini S, Moreira ED, Schmid H, Machado UF. Sympathetic modulation of the renal glucose transporter GLUT2 in diabetic rats. Auton Neurosci 2005;117:54–61
40. Almind K, Kahn CR. Genetic determinants of energy expenditure and insulin resistance in diet-induced obesity in mice. Diabetes 2004;53:3274–3285
41. Obici S, Feng Z, Tan J, Liu L, Karkanias G, Rossetti L. Central melanocortin receptors regulate insulin action. J Clin Invest 2001;108:1079–1085
42. Nogueiras R, Wiedmer P, Perez-Tilve D, et al. The central melanocortin system directly controls peripheral lipid metabolism. J Clin Invest 2007;117:3475–3488
43. Noonan WT, Banks RO. Renal function and glucose transport in male and female mice with diet-induced type II diabetes mellitus. Proc Soc Exp Biol Med 2000;225:221–230
44. Thorens B, Guillam MT, Beermann F, Burcelin R, Jaquet M. Transgenic reexpression of GLUT1 or GLUT2 in pancreatic beta cells rescues GLUT2-null mice from early death and restores normal glucose-stimulated insulin secretion. J Biol Chem 2000;275:23751–23758
45. Grünert SC, Schwab KO, Pohl M, Sass JO, Santer R. Fanconi-Bickel syndrome: GLUT2 mutations associated with a mild phenotype. Mol Genet Metab 2012;105:433–437
46. Ste Marie L, Palmiter RD. Norepinephrine and epinephrine-deficient mice are hyperinsulinemic and have lower blood glucose. Endocrinology 2003;144: 4427–4432
47. Rahmouni K, Haynes WG, Morgan DA, Mark AL. Role of melanocortin-4 receptors in mediating renal sympathoactivation to leptin and insulin. J Neurosci 2003;23:5998–6004
48. Mahfoud F, Schlaich M, Kindermann I, et al. Effect of renal sympathetic denervation on glucose metabolism in patients with resistant hypertension: a pilot study. Circulation 2011;123:1940–1946
49. Schwartz MW, Seeley RJ, Tschöp MH, et al. Cooperation between brain and islet in glucose homeostasis and diabetes. Nature 2013;503:59–66